LIVER DISEASE

Targeting diacylglycerol acyltransferase 2 for the treatment of nonalcoholic steatohepatitis

Neeta B. Amin[1]*, Santos Carvajal-Gonzalez[2], Julie Purkal[1], Tong Zhu[2], Collin Crowley[1], Sylvie Perez[1], Kristin Chidsey[2], Albert M. Kim[1], Bryan Goodwin[1]

Nonalcoholic steatohepatitis (NASH) is characterized by the accumulation of hepatocyte triglycerides, the synthesis of which is catalyzed by diacylglycerol acyltransferases (DGATs). Here, we investigate DGAT2 as a potential therapeutic target using an orally administered, selective DGAT2 inhibitor, PF-06427878. Treatment with PF-06427878 resulted in the reduction of hepatic and circulating plasma triglyceride concentrations and decreased lipogenic gene expression in rats maintained on a Western-type diet. In a mouse model of NASH, histological improvements in steatosis, ballooning, and fibrosis were evident in the livers of animals receiving PF-06427878 compared with mice treated with vehicle alone. We extended these nonclinical studies to two phase 1 studies in humans [NCT02855177 ($n = 24$) and NCT02391623 ($n = 39$; $n = 38$ completed)] and observed that PF-06427878 was well tolerated and influenced markers of liver function (alanine aminotransferase, aspartate aminotransferase, alkaline phosphatase, and total bilirubin) in healthy adults, with statistically significant reductions from baseline at day 14 in participants treated with PF-06427878 1500 milligrams per day ($P < 0.05$). Moreover, magnetic resonance imaging using proton density fat fraction showed that PF-06427878 1500 milligrams per day reduced hepatic steatosis in healthy adult participants. Our findings highlight DGAT2 inhibition by a small, potent, selective compound as a potential therapeutic approach for the treatment of NASH.

INTRODUCTION

Nonalcoholic fatty liver disease (NAFLD) and, more specifically, nonalcoholic steatohepatitis (NASH) are the leading causes of liver disease in the Western world (*1*), with NAFLD affecting about 25% of adults and NASH between 1.5 and 6.5% of adults globally (*2*). Currently, a clinical diagnosis of NASH is established when a liver biopsy exhibits steatosis (the accumulation of fat in the liver), inflammation, and cytological ballooning of liver hepatocytes (*3*), typically accompanied by some degree of fibrosis (*4*). NASH can progress with increasing degrees of fibrosis, at times leading to adverse clinical sequelae such as cirrhosis (*5*) and hepatocellular carcinoma (HCC) (*6*). The pathophysiology of NASH involves steatosis, inflammation, and, ultimately, hepatocyte injury and death (*4*). Steatosis is a key factor in the etiology of NASH (*4*) and is a potential target for therapeutic intervention.

Alterations in lipid metabolism have been hypothesized to contribute to the molecular pathogenesis of NAFLD and NASH (*7*). Diacylglycerol (DAG) acyltransferases (DGATs) catalyze the terminal step in the synthesis of triacylglycerol through the esterification of fatty acyl–coenzyme A (CoA) to DAG (*8*). In mammals, two structurally unrelated DGAT enzymes, DGAT1 and DGAT2, have been characterized: DGAT1 is expressed abundantly in the intestine, where it plays a critical role in the absorption of dietary lipids (*9*), whereas DGAT2 is found in the liver and adipose tissue (*9*) and, unlike DGAT1, exhibits high substrate specificity for DAG (*10*). We have previously shown that pharmacologic blockade of DGAT2 with a selective inhibitor ameliorated hepatic steatosis and improved the circulating lipoprotein profile in low-density lipoprotein receptor knockout mice (*11*), consistent with independent studies of suppression of DGAT2 in genetic and dietary models of metabolic diseases (*12*–*15*).

PF-06427878 is an orally bioavailable, potent, and selective DGAT2 inhibitor, the discovery of which has been reported previously (*16*). We hypothesized that DGAT2 inhibition by PF-06427878 would result in antisteatotic, anti-inflammatory, and antifibrotic effects in murine models. Here, we describe experiments using PF-06427878 in nonclinical models of NAFLD and NASH and characterize the spectrum of effects by quantifying hepatic lipid burden, inflammatory histologic features, stellate cell activation, and extracellular matrix deposition. Furthermore, to assess the therapeutic potential of this mechanism, we investigated whether treatment with PF-06427878 would alter clinically important hepatic biomarkers and liver fat in healthy adults.

RESULTS

Nonclinical characterization of PF-06427878

In vitro characterization of PF-06427878

We determined the in vitro potency of PF-06427878 (the structure of which is shown in fig. S1) for inhibition of DGAT2 by monitoring the incorporation of [1-^{14}C]decanoyl-CoA into [1-^{14}C]tridecanoylglycerol in the presence of 1-2-didecanoyl-*sn*-glycerol and recombinant DGAT2. In this setting, PF-06427878 inhibited human and rat DGAT2 with a half maximal inhibitory concentration (IC_{50}) of 99 and 202 nM, respectively. We assessed the selectivity of PF-06427878 over related acyltransferases, specifically human DGAT1, mouse monoacylglycerol acyltransferase 1 (MGAT1), and human MGAT2 and MGAT3 as described elsewhere (*11*). PF-06427878 demonstrated greater than 470-fold selectivity for DGAT2 over related acyltransferases.

To evaluate the functional effects of PF-06427878 on lipid synthesis in hepatocytes, [^{14}C]glycerol incorporation into triglyceride (TG) was monitored in primary cultures of human hepatocytes. In human hepatocytes, the primary DGAT responsible for TG production

[1]Internal Medicine Research Unit, Pfizer Worldwide Research and Development, Cambridge, MA 02139, USA. [2]Early Clinical Development, Pfizer Worldwide Research and Development, Cambridge, MA 02139, USA.
*Corresponding author. Email: neeta.amin@pfizer.com

is DGAT1 (*11*). To monitor DGAT2 activity, we added a selective DGAT1 inhibitor (PF-04620110) to the culture media to completely inhibit endogenous DGAT1 activity. In this setting, PF-06427878 inhibited human DGAT2 with an IC_{50} of 11.6 ± 1.3 nM (Table 1).

In vivo characterization of PF-06427878

To test the efficacy of PF-06427878 in vivo, we maintained male Sprague-Dawley rats ($n = 56$) on a Western-type diet (WTD) [0.21% (w/w) cholesterol and 40% kcal fat] or standard laboratory chow for 14 days and then orally administered PF-06427878 [0.1 to 30 mg/kg twice daily (BID)] or vehicle alone for 7 days. Compared with animals maintained on standard laboratory chow, animals fed a WTD exhibited increased concentrations of hepatic TGs (2.8-fold; $P < 0.001$; Fig. 1A) and circulating plasma TGs (2.7-fold; $P < 0.001$; Fig. 1B), whereas treatment of WTD-fed rats with PF-06427878 resulted in a dose-dependent reduction in both hepatic and plasma TG concentrations (Fig. 1, A and B, respectively).

On the basis of previous work with other selective DGAT2 inhibitors (*17*) or antisense-mediated knockdown of DGAT2 expression (*14*), it has been demonstrated that, in addition to a direct effect on TG synthesis, inhibition of DGAT2 may indirectly reduce fatty acid synthesis through suppression of genes encoding proteins involved in de novo lipogenesis. It has been suggested that the effect of DGAT2 inhibition on de novo lipogenesis is mediated by indirect suppression of sterol regulatory element binding transcription factor 1c (SREBP1c) (*14*, *15*, *17*). To evaluate this hypothesis, we measured the expression of SREBP1c and its target genes in rats fed a WTD. As expected, induction of obesity caused a fourfold increase ($P < 0.001$; Fig. 1C) in *Srebp1c* mRNA as well as significant increases in acetyl-CoA carboxylase 1 (*Acc1*; 1.6-fold; $P < 0.05$), stearoyl-CoA desaturase 1 (*Scd1*; 24-fold; $P < 0.001$), and fatty acid desaturase 2 (*Fads2*; 1.5-fold; $P < 0.05$; Fig. 1C) mRNA expression. However, treatment of WTD-fed animals with PF-06427878 30 mg/kg BID almost completely normalized *Srebp1c* expression ($P < 0.001$) and significantly reduced *Acc1*, *Scd1*, and *Fads2* expression ($P < 0.01$). The reduction in expression of the fatty acid synthase (*Fasn*) gene did not reach statistical significance ($P = 0.055$; Fig. 1C). Last, the expression of the SREBP1c-target gene, patatin-like phospholipase domain–containing protein 3 (*Pnpla3*), which has a well-documented genetic association with liver fat content (*18*), was suppressed by >90% upon inhibition of DGAT2 ($P < 0.05$; Fig. 1C).

To better understand the TG-lowering effects of PF-06427878, we administered rats poloxamer 407 (a nonionic detergent that blocks the breakdown of TG-rich lipoproteins by lipoprotein lipase) 30 min after oral administration of PF-06427878 (10 mg/kg), the microsomal TG transfer protein (MTP) inhibitor CP-346086 (10 mg/kg), or vehicle alone (0.5% methylcellulose). In fasted or fed animals treated with poloxamer 407, the rate of increase in plasma TG concentrations appears to reflect the rate of hepatic very-low-density lipoprotein TG (VLDL-TG) secretion (*19*). We included the MTP inhibitor CP-346086 as a control for the study, because this compound completely suppresses VLDL-TG secretion (*20*). Before poloxamer 407 administration, PF-06427878 treatment resulted in a rapid reduction in plasma TG concentrations. At baseline (30 min after treatment with PF-06427878), plasma TG concentrations in animals receiving PF-06427878 were 58 ± 8 mg/dl versus 132 ± 31 mg/dl in vehicle-treated animals. At 30 and 60 min after poloxamer 407 dosing, plasma TG concentrations in PF-06427878–treated animals were significantly lower than animals receiving vehicle alone ($P < 0.001$; Fig. 1D). Linear regression analysis showed VLDL-TG secretion rates to be 211 ± 32 mg/dl per hour and 537 ± 80 mg/dl per hour in PF-06427878– and vehicle-treated animals, respectively. This represents a 56% reduction in VLDL-TG secretion rate after treatment with PF-06427878 relative to vehicle. As expected, the MTP inhibitor CP-346086 completely blocked hepatic VLDL secretion (Fig. 1D) (*20*). These data demonstrate that inhibition of DGAT2 with PF-06427878 results in the suppression of hepatic VLDL-TG output.

Because excessive accumulation of lipid in the liver has been postulated to be a prerequisite for the development of NASH (*4*), we also evaluated the effects of PF-06427878 on the development of NASH using the STAM NASH-HCC mouse model. In this model, NASH is induced in male mice by a single subcutaneous injection of streptozotocin 2 days after birth, followed by maintenance on a high-fat diet (HFD) from 4 weeks of age. These mice progressively develop hepatic steatosis and inflammation, hepatocellular ballooning and degeneration, fibrosis, and, ultimately, HCC (*21*). From 5 weeks of age, mice were orally administered PF-06427878 at 2 mg/kg BID (4 mg/kg per day) or 20 mg/kg BID (40 mg/kg per day) or vehicle alone and euthanized at 9 weeks of age. There were no significant differences in mean liver-to-body weight ratio between animals treated with PF-06427878 at 2 or 20 mg/kg BID or vehicle alone (means ± SEM, 6.4 ± 0.11, 6.5 ± 0.32, and 6.5 ± 0.28, respectively; $P > 0.05$).

Treatment of mice with PF-06427878 significantly improved steatosis and hepatocellular ballooning ($P < 0.05$) and suggested a decrease in lobular inflammation (Fig. 2A). As a result, the NAFLD activity score (the sum of steatosis, hepatocellular ballooning, and lobular inflammation scores) (*22*) was significantly reduced in animals treated with PF-06427878 at 2 mg/kg BID (2.3 ± 0.35; $P < 0.001$) and 20 mg/kg BID (1.5 ± 0.32; $P < 0.001$) compared with animals receiving vehicle (5.3 ± 0.32) (Fig. 2B). In addition, treatment with PF-06427878 reduced collagen deposition as determined by Sirius red staining (Fig. 2C). Thus, the percentage of fibrotic area was significantly decreased with PF-06427878 at both 2 mg/kg BID (0.38% ± 0.07; $P < 0.001$) and 20 mg/kg BID (0.68% ± 0.15; $P < 0.01$) compared with vehicle (1.36% ± 0.18). Consistent with observations in the WTD-fed rats, PF-06427878 treatment reduced the expression of multiple lipogenic genes, including *Srebp1c*, *Acc1*, *Fasn*, *Scd1*, and *Pnpla3* in the STAM model (Fig. 2D).

To further investigate the molecular mechanisms underlying the histopathological improvements outlined above, we profiled the expression of genes involved in hepatic stellate cell activation and regulation of fibrosis [transforming growth factor–β (*Tgfb*) and interferon-γ (*Ifng*)] (*23*), extracellular matrix deposition and remodeling [collagen type I α2 chain (*Col1a2*) and matrix metallopeptidase 2 (*Mmp2*)] (*23*, *24*), as well as a marker of stellate cell activation [actin α2, smooth muscle (*Acta2*)] (*25*). In agreement with the reductions in Sirius red staining of the liver, the expression of the gene encoding *Col1a2* was significantly reduced after PF-06427878 treatment ($P < 0.05$; Fig. 2E). In addition, PF-06427878 treatment significantly increased the expression of *Ifng* ($P < 0.05$; Fig. 2E), which is notable because interferon-γ has been previously reported to block extracellular matrix deposition in a rat liver model of fibrosis (*26*). There were no significant changes in the expression of genes encoding *Acta2* or profibrogenic cytokine *Tgfb* ($P > 0.05$; Fig. 2E).

When the effects of PF-06427878 on fasting plasma lipids were evaluated, PF-06427878 treatment significantly reduced total cholesterol (TC) concentrations, compared with vehicle ($P < 0.05$; table S1). There was a numerical increase in β-hydroxybutyric acid

Table 1. Summary of in vitro pharmacologic activity and nonclinical and clinical pharmacokinetic properties of PF-06427878. F_a determined after 10 mg/kg of oral dose in 0.5% methylcellulose. CYP, cytochrome P450; DGAT1, diacylglycerol acyltransferase 1; DGAT2, diacylglycerol acyltransferase 2; IC_{50}, half maximal inhibitory concentration; MGAT1, monoacylglycerol acyltransferase 1; MGAT2, monoacylglycerol acyltransferase 2; MGAT3, monoacylglycerol acyltransferase 3; AUC_{inf}, area under the plasma concentration time profile from 0 extrapolated to infinity; AUC_{last}, area under the plasma concentration time profile from 0 to the last quantifiable concentration; AUC_{tau}, area under the plasma concentration time profile from time 0 to time tau (τ), where τ equals 8 hours; C_{max}, maximum plasma concentration; CV, coefficient of variation; *n*, number of participants in the treatment group and contributing to the summary statistics; *n*1, number of participants for AUC_{inf} and $t_{1/2}$; NA, not applicable; NR, not reported; PK, pharmacokinetics; Q8H, every 8 hours; $t_{1/2}$, terminal elimination half-life; T_{max}, time for C_{max}.

Assay	Pharmacodynamic activity
Recombinant enzyme inhibition assays: DGAT2	
Human DGAT2, IC_{50} (nM)	99.9 ± 3.2*
Rat DGAT2, IC_{50} (nM)	202 ± 4.4*
Recombinant enzyme inhibition assays: Selectivity	
Human DGAT1, IC_{50} (μM)	>50
Mouse MGAT1, IC_{50} (μM)	>50
Human MGAT2, IC_{50} (μM)	>45
Human MGAT3, IC_{50} (μM)	>50
Primary hepatocyte assays	
Human DGAT2, IC_{50} (nM)	11.6 ± 1.3*
Nonclinical pharmacokinetic properties	
Fraction unbound (F_u), human/rat plasma	0.046/0.038
Fraction absorbed in rat, F_a (%)	78.0
Total plasma clearance, rat, CLp (ml/min per kg)	31.4
Human CYP1A2, CYP2B6, CYP2C9, CYP2C19, CYP2D6, and CYP3A4/5 inhibition, IC_{50} (μM)	>100

*Means ± SEM

Clinical pharmacokinetic properties

	n, *n*1	C_{max} (ng/ml)	T_{max} (hours)	$t_{1/2}$ (hours)	AUC_{inf} (ng·hour/ml)	AUC_{tau} (ng·hour/ml)
Single ascending doses of PF-06427878*						
3 mg	6, 1	6.3 (48)	2.0 (0.5–3.0)	NR	NR	NA
10 mg	6, 4	25.5 (74)	1.5 (0.5–3.0)	1.6 ± 0.3	81.4 (49)	NA
30 mg	6, 6	72.0 (30)	2.0 (0.5–4.0)	1.7 ± 0.2	242.0 (20)	NA
100 mg	6, 6	244.1 (26)	3.1 (0.5–4.0)	3.0 ± 0.9	870.2 (57)	NA
300 mg	6, 3	1092 (28)	1.5 (1.0–4.0)	5.2 ± 1.7	3046† (37)	NA
600 mg	6, 5	1728 (41)	2.0 (1.0–2.0)	4.4 ± 2.2	5867† (33)	NA
1200 mg	6, 5	4072 (34)	2.0 (0.5–4.0)	5.3 ± 2.2	17940† (21)	NA
2000 mg	6, 5	9302 (63)	4.0 (3.0–6.0)	5.0 ± 1.0	43830† (41)	NA
Multiple doses of PF-06427878 with plasma PK assessed on day 14*,‡						
15 mg/day	6, 1	11.2 (43)	1.0 (1.0–1.0)	NR	NR	21.5 (67)
45 mg/day	8, 4	39.0 (44)	1.0 (1.0–2.1)	7.6 ± 3.7	NR	109.0 (40)
150 mg/day	8, 2	127.5 (51)	1.0 (1.0–3.0)	NR	NR	299.8 (54)
450 mg/day	8, 5	476.4 (72)	1.0 (1.0–2.0)	10.3 ± 3.4	NR	1208 (63)
1500 mg/day	12, 10	1254 (69)	1.0 (0.5–3.9)	6.2 ± 2.4	NR	4403 (54)

*Geometric mean (%CV) for all PK parameters except: median (range) from T_{max}; arithmetic means ± SD for $t_{1/2}$. †The mean value of AUC_{last} was higher than AUC_{inf} when AUC_{inf} was not reportable in individual participant(s) with high AUC_{last} value(s). ‡Daily administration divided Q8H with a meal.

in animals treated receiving PF-06427878 compared with animals receiving vehicle ($P > 0.05$). No differences in plasma TG concentrations were observed between treatment groups (table S1).

Representative photomicrographs of the hematoxylin and eosin (H&E)–stained sections are shown in Fig. 3A. Vehicle-treated animals exhibited micro- and macrovesicular fat deposition, hepatocellular

ballooning, and inflammatory cell infiltration, all of which were reduced in mice receiving PF-06427878 at 20 mg/kg BID. Although these representative images did not show inflammatory cell infiltration, we noted a reduction in lobular inflammation (Fig. 3A). Sirius red staining of liver sections showed perivenular and perisinusoidal collagen deposition in the pericentral regions of the liver lobule in vehicle-treated animals; in contrast, treatment with PF-06427878 markedly reduced collagen deposition in the pericentral region compared with animals treated with vehicle alone (Fig. 3B).

Collectively, our in vitro and in vivo data from two rodent NASH-related models demonstrate that inhibition of DGAT2 with PF-06427878 reduced hepatic lipid burden, improved histopathology, and decreased stellate cell activation and deposition of extracellular matrix. The weight of this evidence supported further evaluation of PF-06427878 in the clinic.

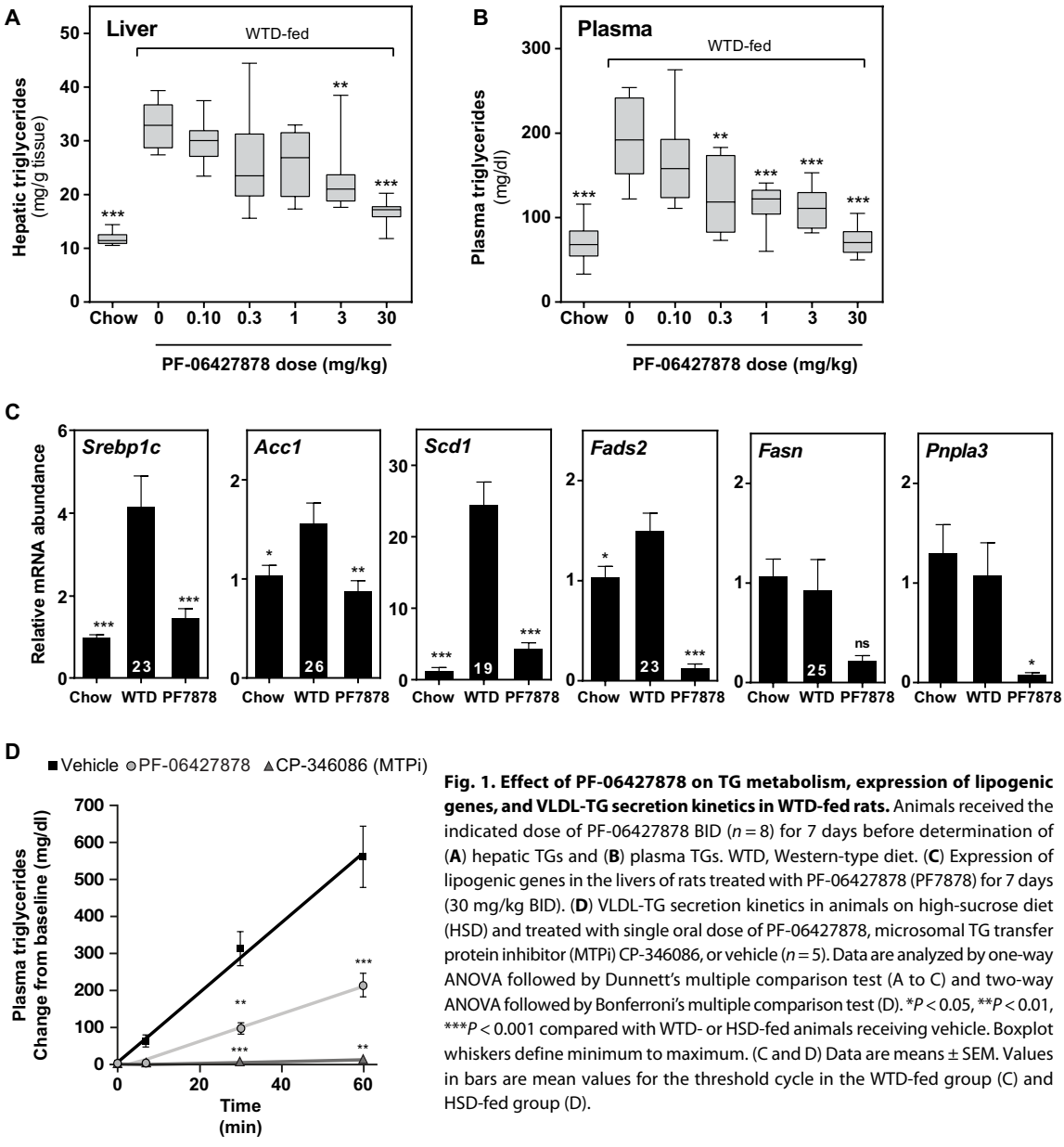

Fig. 1. Effect of PF-06427878 on TG metabolism, expression of lipogenic genes, and VLDL-TG secretion kinetics in WTD-fed rats. Animals received the indicated dose of PF-06427878 BID ($n = 8$) for 7 days before determination of (**A**) hepatic TGs and (**B**) plasma TGs. WTD, Western-type diet. (**C**) Expression of lipogenic genes in the livers of rats treated with PF-06427878 (PF7878) for 7 days (30 mg/kg BID). (**D**) VLDL-TG secretion kinetics in animals on high-sucrose diet (HSD) and treated with single oral dose of PF-06427878, microsomal TG transfer protein inhibitor (MTPi) CP-346086, or vehicle ($n = 5$). Data are analyzed by one-way ANOVA followed by Dunnett's multiple comparison test (A to C) and two-way ANOVA followed by Bonferroni's multiple comparison test (D). $^*P < 0.05$, $^{**}P < 0.01$, $^{***}P < 0.001$ compared with WTD- or HSD-fed animals receiving vehicle. Boxplot whiskers define minimum to maximum. (C and D) Data are means ± SEM. Values in bars are mean values for the threshold cycle in the WTD-fed group (C) and HSD-fed group (D).

Toxicology studies with PF-06427878

Beyond the doses of PF-06427878 evaluated in our pharmacology studies, we also conducted 2-week toxicology studies with PF-06427878 at doses up to 1000 mg/kg per day (in Wistar Han International Genetic Standardization rats) and up to 500 mg/kg per day (in cynomolgus monkeys). In rats, there was no effect on alanine aminotransferase (ALT), aspartate transaminase (AST), or alkaline phosphatase (ALP) concentrations (fig. S2). In monkeys, although we noted changes in mean response (both increases and decreases relative to vehicle), there was a lack of consistency in change across the circulating markers of liver function (fig. S2). In both species, no adverse effects in the bone were apparent.

Clinical investigation of PF-06427878 in healthy adults

Participants and study design

We evaluated the initial safety and tolerability of oral dosing of PF-06427878 in three phase 1 clinical studies, all in healthy adults (≥18 years of age): B7871001 [NCT02208284, single-dose study in participants with a body mass index (BMI) of 17.5 to 35.4 kg/m^2], B7871002 (NCT02391623, multiple-dose study in those with a BMI of 17.5 to 35.4 kg/m^2), and B7871005 (NCT02855177, multiple-dose study in those with a BMI of ≥25 kg/m^2). The results presented here are from the latter two studies.

In study B7871002, a total of 39 participants were randomized to receive placebo or PF-06427878 at doses of 15, 45, 150, or 450 mg/day [daily administration divided every 8 hours (Q8H), with a meal; fig. S3A] for 14 days [mean age, 35.7 years (range, 23 to 54); mean BMI, 27.2 kg/m^2 (range, 21.5 to 35.1 kg/m^2); white, $n = 35$; black, $n = 2$; Asian, $n = 1$; and other, $n = 1$]. One participant in the PF-06427878 450 mg/day cohort discontinued the study on day 6, for nonsafety reasons; data from all randomized participants were analyzed for safety and pharmacodynamics. In study B7871005, 24 participants were randomized to receive placebo or PF-06427878

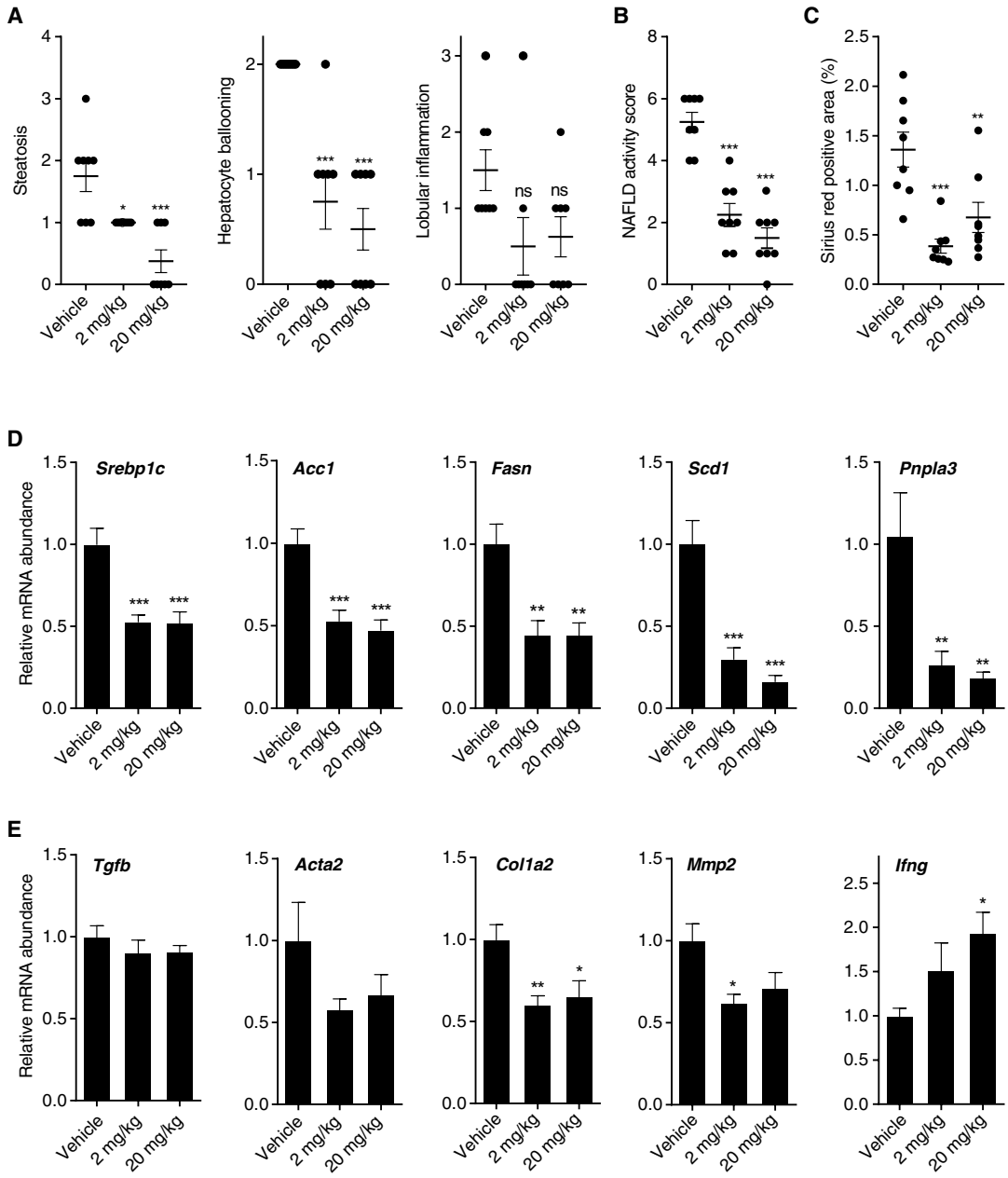

Fig. 2. Effects of PF-06427878 on the development of liver disease in a STAM NASH-HCC mouse model. After the induction of NASH, mice were administered PF-06427878 at 2 mg/kg BID (4 mg/kg per day) or 20 mg/kg BID (40 mg/kg per day) or vehicle alone for 4 weeks and euthanized at 9 weeks of age. (**A**) Histopathological scoring of hepatic steatosis, hepatocellular ballooning, and lobular inflammation. (**B**) Calculated NAFLD activity score. (**C**) Sirius red staining was used to quantitate collagen deposition in the liver. (**D**) Expression of multiple lipogenic genes in the liver. (**E**) Expression of genes involved in hepatic stellate cell activation, regulation of fibrosis, myofibroblast function, and extracellular matrix deposition and remodeling in the liver. Data are presented as means ± SEM with $n = 8$ animals per group. All data are analyzed by one-way ANOVA followed by Dunnett's multiple comparison compared with vehicle. $^{*}P < 0.05$, $^{**}P < 0.01$, $^{***}P < 0.001$. ns, not significant.

1500 mg/day (daily administration divided Q8H) (fig. S3B) for 14 days [mean age, 44.4 years (range, 28 to 55); mean BMI, 33.7 kg/m^2 (range, 26.3 to 44.7 kg/m^2); white, n = 22; Asian, n = 1; and other, n = 1]; with all participants' data analyzed for safety and pharmacodynamics.

Safety and tolerability

More than the 100-fold dose range was evaluated across studies B7871002 and B7871005 (15 to 1500 mg/day), PF-06427878 was generally well tolerated, and only infrequent adverse events were observed (Table 2). There was no evidence of adverse effects on cardiac conduction (assessed via serial 12-lead electrocardiograms) or blood pressure. On the basis of plasma exposure–response analysis for doses up to 450 mg/day (study B7871002), an average increase in the heart rate of eight beats per minute at 1 hour on day 14 with the highest exposures was observed.

Impact on the liver

Treatment with PF-06427878 in healthy humans influenced liver function tests. Figure 4 summarizes the changes from baseline in ALT, AST, ALP, and the total bilirubin (TBILI) observed in studies B7871002 and B7871005 after 14 days of repeated dosing of PF-06427878 (15 to 1500 mg/day). For each of these markers of liver function, we observed a significant reduction from baseline relative to placebo in participants treated with the highest PF-06427878 dose, 1500 mg/day, in study B7871005 ($P < 0.05$ for all markers). At this dose, the median change from baseline observed was −9.0 U/liter (ALT), −4.5 U/liter (AST), −17 U/liter (ALP), and −0.2 mg/dl (TBILI) compared with 0.0 U/liter (ALT), −1.5 U/liter (AST), −2.5 U/liter (ALP), and 0 mg/dl (TBILI) with placebo (Fig. 4). Note that there was a mean decrease relative to placebo in ALT, AST, and ALP with all PF-06427878 doses; however, for ALT and AST, these changes did not reach statistical significance at doses below 1500 mg/day ($P > 0.05$). For ALP, doses of ≥45 mg/day showed significant reductions ($P < 0.05$) using the Williams test for multiple comparisons to placebo.

The effects of PF-06427878 on serum TGs were inconsistent in the phase 1 studies. In study B7871002, the mean reduction in TGs was greater than placebo with all PF-06427878 doses with a statistically significant reduction observed with PF-06427878 150 mg/day versus

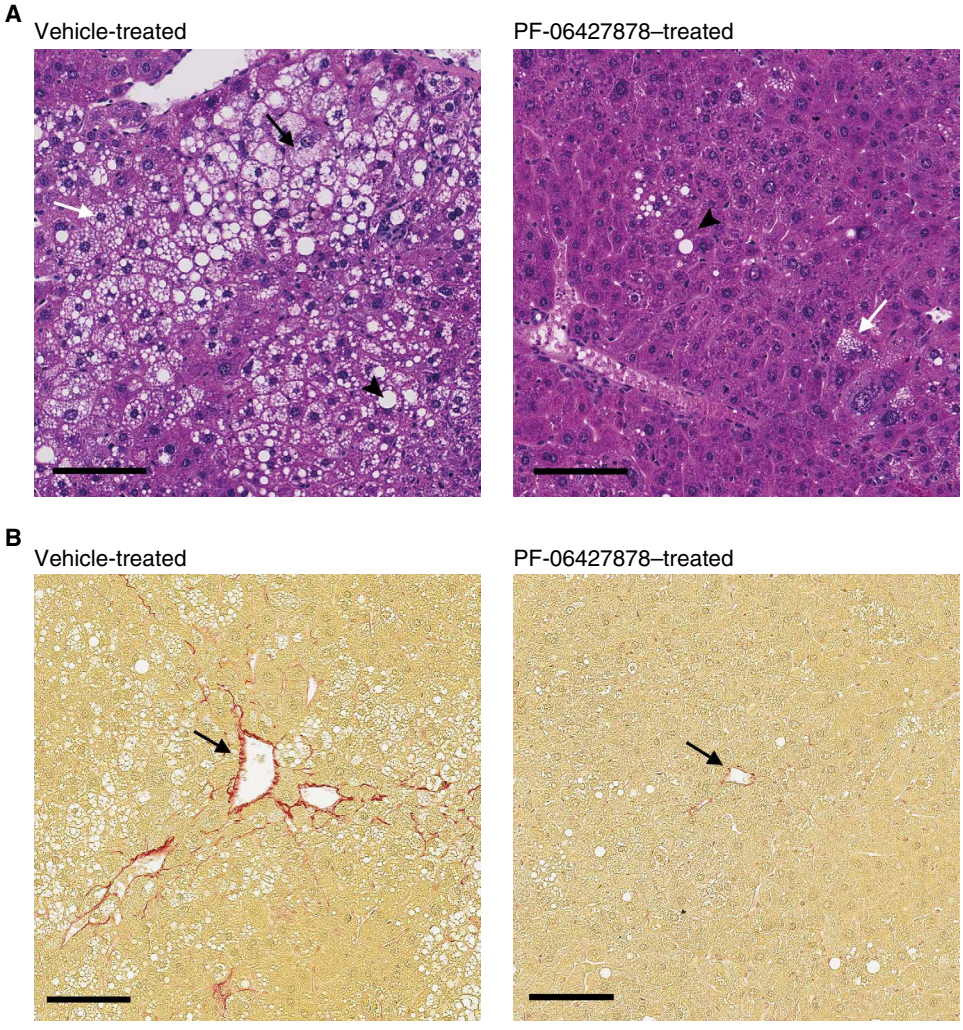

Fig. 3. Representative photomicrographs of H&E- and Sirius red–stained sections in a STAM NASH-HCC mouse model. After the induction of NASH, mice were administered PF-06427878 at 2 mg/kg BID (4 mg/kg per day) or 20 mg/kg BID (40 mg/kg per day) or vehicle alone for 4 weeks ($n = 8$ animals per group) and euthanized at 9 weeks of age. Livers were collected for histopathological analysis. Sections were cut from paraffin blocks of liver tissue prefixed with Bouin's solution and stained with H&E or Sirius red. (**A**) H&E stain of the liver from vehicle- and PF-06427878–treated mice. Micro- and macrovesicular lipid deposition in hepatocytes are shown by the white arrow and black arrowhead, respectively; ballooning degeneration of hepatocytes is shown by the black arrow. Scale bars, 100 μm. (**B**) Sirius red stain liver sections from vehicle- and PF-06427878–treated mice. Reductions in perivenular collagen are shown by black arrows. Scale bars, 100 μm.

placebo ($P < 0.05$). However, in study B7871005, PF-06427878 at a dose of 1500 mg/day was not observed to have a significant effect on fasting or postprandial TG concentrations compared with placebo ($P > 0.05$; Table 3).

The effects of PF-06427878 on serum lipids in the clinical studies were less consistent than those observed in the nonclinical studies. Dosing with PF-06427878 more than 2 weeks with doses of ≤450 mg/day (study B7871002) did not result in consistently monotonic changes in the standard serum lipid panel, including direct low-density lipoprotein cholesterol (LDL-c), high-density lipoprotein cholesterol (HDL-c), or TC measured at day 14 (table S2). However, at the highest dose tested in the separate study, B7871005, PF-06427878 1500 mg/day produced significant reductions in direct LDL-c and HDL-c ($P < 0.05$; table S2).

In addition to safety and tolerability, study B7871005 also assessed the potential clinical antisteatotic effect of PF-06427878 in healthy adults by measuring change in liver fat compared with baseline, as reported by magnetic resonance imaging–based proton density fat fraction (MRI-PDFF), on day 15. Treatment with PF-06427878 markedly reduced liver fat by an average 31.5% (80% confidence interval: −42.2 to −18.7) after adjusting for placebo response (Fig. 5 and fig. S4).

DISCUSSION

NAFLD and NASH are increasingly visible disease entities that lack approved pharmacotherapies (*1*), and their prevalence is expected to increase, fueled by population trends in obesity (*27*) and the metabolic syndrome (*28*, *29*). Steatosis is a fundamental step in the pathogenesis of these conditions, and our prior experience with DGAT2 pharmacologic blockade implicated a potential therapeutic role for DGAT2 inhibition in NAFLD and NASH (*11*). Prior work has documented the discovery of DGAT1 inhibitors (*30*–*32*) and of DGAT2 inhibitors in a nonclinical setting (*11*, *15*, *33*, *34*). Here, we characterized the effects of a small-molecule DGAT2 inhibitor in both nonclinical and clinical settings.

As we present here, PF-06427878 is a highly selective and potent DGAT2 inhibitor, based on its in vitro characterization and dose-dependent inhibition of triacylglycerol synthesis. The potency of PF-06427878 appeared higher in the cellular assay (11.2 nM), compared with the biochemical assay (91.6 nM). The reason for this variation remains unclear; however, it may be due to active transporter-mediated uptake to the cell increasing the relative intracellular concentration or because the compound exhibits time-dependent inhibition of DGAT2 in vitro, as has been observed with a previously characterized DGAT2 inhibitor (PF-06424439) (*35*). In vivo studies in WTD-fed rats verified that PF-06427878 treatment reduced both the liver and plasma TGs. In line with earlier studies using a structurally unrelated compound (*34*), we showed that PF-06427878 could directly lower circulating TG concentrations through suppression of VLDL secretion. In addition to these direct effects on circulating lipids, PF-06427878 treatment of rats resulted in decreased expression of genes encoding proteins involved in de novo lipogenesis. Together, these data indicate that PF-06427878 modulates hepatic lipid metabolism through its direct effects on DGAT2-mediated TG synthesis and indirectly through suppression of genes involved in de novo lipogenesis.

Table 2. Adverse events reported by two or more healthy adult participants after repeated oral dosing of a range of PF-06427878 doses in humans (studies B7871002 and B7871005).

	Placebo*	PF-06427878 dose per day (administration divided Q8H with a meal)				
		15 mg	45 mg	150 mg	450 mg	1500 mg
Number of participants per group	20	6	8	8	9	12
BMI, kg/m^2, median (range)	31.0 (24.6–44.7)	26.1 (24.0–27.6)	24.8 (21.4–30.2)	26.8 (23.6–35.1)	27.6 (25.5–31.5)	33.8 (27.1–40.2)
Number of healthy adult participants with specific adverse events						
Diarrhea	2	0	1	0	2	0
Abdominal pain	2	0	1	1	0	0
Headache	2	0	1†	1†	0	0
Dyspepsia	2	0	0	1	0	0
Nasal dryness	1	0	2	0	0	0
Constipation	0	1	0	0	1	1
Flatulence	0	0	2	0	0	0
Gastroenteritis	1†	0	0	0	1†	0

*Combining participants randomized to placebo in study B7871002 ($n = 8$) and B7871005 ($n = 12$). †Adverse event of moderate intensity; all other adverse events were mild in intensity.

These findings were extended in the context of STAM NASH-HCC mice, where DGAT2 inhibition by PF-06427878 resulted in a substantial decline in the histology-based NAFLD activity score, reflecting advantageous cellular-level changes in hepatic steatosis, hepatocellular ballooning, and lobular inflammation. Moreover, mRNA expression patterns were consistent with these cellular effects, revealing notable changes in the expression of genes regulating lipid synthesis (*Pnpla3*), tissue remodeling (*Mmp2*), and fibrosis (*Ifng*). The beneficial effects of DGAT2 inhibition on liver fibrosis observed here are in contrast with a previous report using a DGAT2 antisense oligonucleotide (ASO), where reduction of hepatic DGAT2 protein expression was associated with increased fibrosis in diabetic (db/db) mice fed a methionine- and choline-deficient diet (*12*). It is not clear as to why we see these differences, but one could speculate that it may be related to the model (STAM versus methionine- and choline-deficient diet) or the manner in which DGAT2 inhibition was achieved (small molecule versus ASO).

One theoretical concern of targeting DGAT2 as a therapeutic strategy is that inhibition of this enzyme would cause the accumulation of potentially toxic liver precursors. In previous studies, we and others found that blockade of DGAT2 reduced the de novo synthesis of fatty acids in rodents (*16*, *34*), which could be attributed to a decline in active SREBP1c. Here, we show that pharmacological inhibition of DGAT2 in rodents also indirectly lead to a reduction in SREBP1c activity as assessed by the expression of its lipogenic target genes. Although the molecular mechanism underlying the indirect suppression of SREBP1c is presently unknown, it is likely that the suppression of de novo lipogenesis contributes to the effects of PF-06427878 on liver fat. Inhibition of DGAT2 has also been shown to redistribute lipid droplets from large to small in rodent hepatocytes (*17*), which could facilitate increased lipid mobilization and further contribute to the observed liver fat reduction after PF-06427878 treatment. Overall, the spectrum of nonclinical data collected for PF-06427878 was directionally consistent in counteracting the pathophysiology of NAFLD/NASH and supported progression to clinical investigation.

In phase 1 clinical testing, we found that PF-06427878 was generally well tolerated and showed promising effects on circulating hepatic biomarkers of liver injury and liver fat. Compared with placebo, PF-06427878 1500 mg/day led to significant reductions of both ALT and AST in humans ($P < 0.05$). Elevated ALT and AST concentrations are recognized as typical hallmarks of the whole spectrum of NAFLD (*36*, *37*). Furthermore, evidence suggests that as fibrosis progresses in patients with NASH, AST concentrations further increase with a resultant rise in the AST:ALT ratio (*38*). Reduction in these markers may therefore be indicative of the beneficial role that DGAT2 inhibition could have in the treatment of NAFLD and NASH. On the other hand, it is unclear why a marked reduction in ALP concentrations observed in the clinic was not seen in the nonclinical studies, including at very high doses of PF-06427878 evaluated in the toxicology studies. This discordance suggests that DGAT2 inhibition with PF-06427878 may induce hepatic effects that are specific to or different between species.

Limited data from clinical studies testing DGAT inhibitors are available. The DGAT1 inhibitor pradigastat is the most widely studied: Early clinical investigation explored its potential for the treatment of hypertriglyceridemia (*39*) and NAFLD (*40*). In these reports, although pradigastat reduced plasma TG concentrations, it also resulted in a high frequency of gastrointestinal adverse events, including diarrhea and nausea (*40*, *41*). Similar reductions in serum TG concentrations accompanied with intolerable gastrointestinal adverse events are reported with another DGAT1 inhibitor, AZD7687 (*42*). In contrast, in our experience, the DGAT2 inhibitor PF-06427878 did not result in clear serum TG reduction but was well tolerated without an increased incidence of gastrointestinal adverse events, compared with placebo, even at doses up to 1500 mg/day. The reason

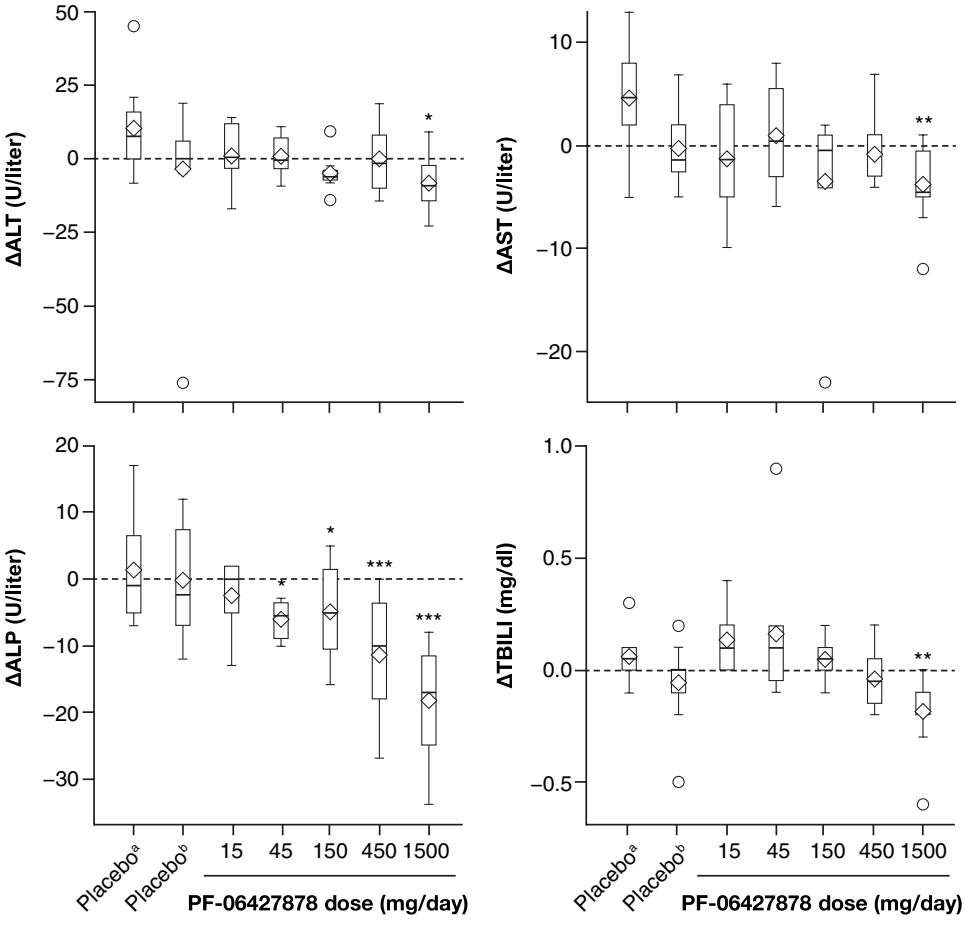

Fig. 4. Liver function tests on day 14 relative to baseline after multiple doses of placebo or PF-06427878 in healthy humans (studies B7871002 and B7871005). The boxplot includes median (horizontal line within box) and arithmetic mean (large open diamond within box), with 25th and 75th percentiles and whiskers to the last point within the 1.5× interquartile range and outliers in open circles. Baseline is defined as the predose measurement on day 1. PF-06427878 15, 45, 150, 450, and 1500 mg/day: $n = 8$, 12, 6, 8, 8, 8, and 12, respectively. *$P < 0.05$, **$P < 0.01$, ***$P < 0.001$, Williams' test. Δ, change from baseline; Placebo[a], study B7871002; Placebo[b], study B7871005.

for these divergent profiles is not clear, but disparate relative tissue expression for these enzymes [high intestinal expression for DGAT1 (*43*) versus the liver for DGAT2 (*10*)] and different molecular properties of the therapeutic candidates, for example, volume of distribution or distinction in the clinical relevance of inhibiting DGAT1 versus DGAT2, may contribute to the discrepancy in findings. The lack of clinical translation for the effect of PF-06427878 on circulating TGs suggests potential differences in the consequences of DGAT2 inhibition in rodents versus humans.

In humans, changes in other fasting serum lipid markers were generally of low magnitude and did not consistently differ when comparing PF-06427878 doses with placebo. An exception was HDL-c, for which PF-06427878 at doses of 45, 150, and 1500 mg/day resulted in a placebo-adjusted decline from a baseline of 11.3, 13.8, and 14.6%, respectively ($P < 0.05$). This observation aligns with genetic reports that a loss-of-function mutation in DGAT2 (Tyr285X) is associated with decreased HDL-c in humans (*44*). The clinical implications of this degree of HDL-c reduction in patients with NASH are unknown. NASH resolution was associated with modest increases in HDL-c (~6%) in a post hoc analysis of the Placebo for the Treatment of Non-Diabetic Patients with Nonalcoholic Steatohepatitis (PIVENS) study (*45*). However, in a recent large study, favorable changes in lipoprotein concentrations, including much larger increases in HDL-c (up to 133%) with the cholesteryl ester transfer protein inhibitor evacetrapib, were not associated with benefits for cardiovascular end points (*46*). Longer interventional studies are necessary to better understand the risk-benefit profile of DGAT2 inhibition for specific patient populations.

Few data are publicly available documenting the clinical effect of DGAT1 inhibition on liver fat. In one clinical study, pradigastat led to a 2.9% reduction compared with placebo after 24 weeks of treatment at the 20-mg dose level (titrated up from 10 mg) (*40*). In comparison, we observed a 31.5% placebo-adjusted reduction in liver fat when administering PF-06427878 at a dose of 1500 mg/day over just 2 weeks. Furthermore, in a 13-week clinical study in patients with type 2 diabetes mellitus and MRI-PDFF of ≥10% at baseline, patients receiving once-weekly 250-mg subcutaneous injection of IONIS-DGAT2$_{RX}$ achieved 26.4% reduction in liver fat (versus those on placebo who were noted to have an increase in liver fat by 1%) (*47*). Although differences between these studies exist in the patient populations, likely different levels of target engagement at the doses studied, duration of treatment, and imaging methodologies, the data from these studies support the inference that DGAT2 inhibition can induce a more marked reduction of liver fat than DGAT1 inhibition.

The robust effect on liver fat in humans after only 2 weeks of pharmacological intervention with PF-06427878 has not been previously reported. Within a comparable treatment period, peroxisome proliferator-activated receptor δ (PPARδ) agonist reduced liver fat by 20%, whereas a PPARα agonist had no effect in moderately obese men (*13*). However, marked reduction in liver fat has been seen in humans on an isocaloric low-carbohydrate diet in as little as 14 days (*48*).

Although no histological assessments of hepatic steatosis were conducted in the clinical study reported here, our assessments of liver fat using MRI-PDFF indicate the robust antisteatotic effects of PF-06427878 in humans. Magnetic resonance quantification of steatosis is now a validated tool for the clinical assessment of hepatic steatosis (*5*), with MRI-PDFF quantification of liver fat shown to significantly correlate with grade of steatosis determined by liver biopsy (*49*, *50*).

There are a number of limitations that apply to the current work. The molecule we used, PF-06427878, is a candidate drug whose chemical properties were not fully optimized for consistent, chronic

Table 3. Effect of repeated oral dosing of PF-06427878 on serum fasting (studies B7871002 and B7871005) and postprandial (study B7871005) TG concentrations in humans. Data are presented from studies B7871002 and B7871005 separately to showcase the effect with increasing doses of PF-06427878 with comparison to within-study placebo. Daily administration of PF-06427878 was divided Q8H with a meal. CI, confidence interval; LS, least squares; and TG, triglycerides.

Dose (mg/day)	*n*	% Change from baseline		Placebo-adjusted % change from baseline		
		Adjusted geometric LS means	80% CI	Adjusted geometric LS means	80% CI	*P*
Fasting serum TG concentrations						
Study B7871002						
Placebo	8	−0.9	−10.1 to 9.2	—	—	—
PF-06427878, 15 mg	6	−8.2	−17.9 to 2.7	−7.3	−20.1 to 7.5	0.5086
PF-06427878, 45 mg	8	−5.4	−14.2 to 4.2	−4.5	−16.8 to 9.5	0.6608
PF-06427878, 150 mg	8	−22.5	−29.7 to −14.6	−21.8	−31.8 to −10.3	0.0254
PF-06427878, 450 mg	8	−9.5	−17.9 to −0.3	−8.7	−20.38 to 4.7	0.3928
Study B7871005						
Placebo	12	−24.5	−34.4 to −13.1	—	—	—
PF-06427878, 1500 mg	12	−16.4	−27.3 to −3.8	10.8	−9.2 to 35.0	0.5034
Postprandial TG concentrations						
Study B7871005						
Placebo	12	−21.0	−29.9 to −10.9	—	—	—
PF-06427878, 1500 mg	12	−20.0	−29.4 to −9.2	1.3	−14.9 to 20.5	0.9236

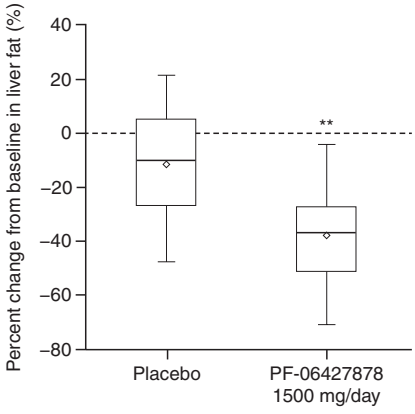

Fig. 5. Reductions in liver fat on day 15 relative to baseline after multiple doses of placebo or PF-06427878 in humans (study B7871005). Reductions in liver fat were assessed using MRI-PDFF. Boxplot includes median (horizontal line within box) and arithmetic mean (solid diamond within box), with 25th and 75th percentiles and whiskers to last point within 1.5× interquartile range, with baseline defined as value as assessed on day −1 ($n = 12$ per group). *P* values were calculated from the differences between placebo and active treatment group LS means in the logarithmic scale. $^{**}P < 0.01$.

exposure in relevant patient populations, and hence, clinical development of this candidate has been discontinued despite promising data. Furthermore, rodent models are incomplete representations of human disease, and their findings may not be extensible to other models or animal species. In addition, we did not assess the effects of PF-06427878 on active SREBP protein expression in WTD-fed rats. However, previous publications have demonstrated that ASO-mediated blockade of DGAT2 signaling results in the suppression of SREBP signaling and decreased expression of SREBP1 target genes (*14*). Moreover, it has previously been shown that pharmacologic inhibition of DGAT2 with a potent and selective small molecule unrelated to PF-06427878 leads to suppression of SREBP1 signaling in a cell-autonomous manner in primary cultures of hepatocytes (*17*). Conversely, overexpression of DGAT2 in the liver increases SREBP1 signaling (*51*). Thus, although the molecular mechanisms underlying these observations are unclear, the link between DGAT2 activity and SREBP signaling has been established. The nonclinical data presented here are consistent with these earlier reports; therefore, it could be hypothesized that PF-06427878 might have similar effects on SREBP signaling.

Limitations also apply to our clinical studies. First, the studies were of limited size and enrolled healthy adult participants, and the results may inadequately reflect treatment response in larger studies in patient populations. Furthermore, the lack of statistical significance in liver function tests with lower doses of PF-06427878 may be due to the limited sample size and lack of power for these comparisons. Hence, although the distinct changes in liver fat and accompanying reductions in liver function tests we observed in the clinical studies reflect the potential of DGAT2 inhibition, further studies with a potent, selective inhibitor of DGAT2 administered for longer duration than in our studies are required to confirm this hypothesis.

In summary, we report our early experience with the small-molecule DGAT2 inhibitor, PF-06427878, which resulted in broadly beneficial effects when administered in animal models relevant to NAFLD and NASH. Early clinical observations were notable for a good tolerability profile and substantial reduction in liver fat after only 2 weeks of administration in healthy adults. Our findings support a

beneficial role for DGAT2 inhibition in rodent models of NAFLD and NASH and demonstrate clinical translation for the reduction of hepatic fat, highlighting DGAT2 inhibition via a small, potent, highly selective compound as a potential therapeutic target for the treatment of NAFLD and NASH.

MATERIALS AND METHODS

Study design

Nonclinical studies

WTD rat model. The purpose of the Western diet experiment was to create an efficacy model for the DGAT2 pathway. Sprague-Dawley rats (180 to 200 g body weight; Envigo) were maintained on a high-fat, high-cholesterol WTD (D12079b, Research Diets) for 2 weeks before being randomized to receive orally administered PF-06427878 (0.1 to 30 mg/kg BID) or vehicle alone (0.5% methylcellulose in sterile reverse osmosis deionized water) for 7 days. Treatment was administered in a blinded manner in the a.m. and p.m., with an 8-hour separation period. Animals received the final dose of PF-06427878 2 hours before blood collection from the lateral tail vein for plasma TG analysis. Animals were euthanized 2 hours after compound administration by means of CO_2 asphyxiation, and the liver was excised, snap-frozen in liquid nitrogen, and held at −80°C until processing. The liver was pulverized in a liquid nitrogen bath for further processing of mRNA and hepatic TGs. Further details on the methods used for mRNA isolation and hepatic TG quantification are given in the Supplementary Materials.

Poloxamer challenge rat model. To better understand the hepatic TG secretion mechanism, we conducted VLDL-TG assessment using Jugular vein cannulated male Wistar rats (200 to 225 g), obtained from Charles River Laboratories and maintained under standard laboratory conditions with a 12-hour light/12-hour dark cycle (lights on at 6:00). For 2 days, before the study, rats were fed a high-sucrose, low-fat diet (TD.03045). On the day of the study, animals were fasted for 4.5 hours before oral administration of PF-06427878 (10 mg/kg), an MTP inhibitor (CP-346086; 10 mg/kg) (*18*), or vehicle alone (0.5% methylcellulose). After a further 30 min, animals were infused with poloxamer 407 [7% (v/v), 10 ml/kg) through the indwelling catheter. Blood was drawn 7, 30, 60, and 120 min after poloxamer 407 dose from the lateral vein and plasma TG concentrations were determined. After linear regression analysis, VLDL-TG secretion rates (milligram per deciliter per hour) were determined from the slope of plasma TG concentrations versus time between 0 and 60 min.

STAM NASH-HCC mouse model. To assess the DGAT2 mechanism efficacy in a more severe NAFLD/NASH model, we performed the STAM NASH-HCC mouse model by Stelic Institute & Co. Pathogen-free 15-day pregnant C57BL/6 mice were obtained from Charles River Laboratories Japan Inc., and NASH was induced in male offspring by a single subcutaneous injection of 200 μg of streptozotocin (Sigma-Aldrich) 2 days after birth, followed by ad libitum HFD (57% kcal fat; HFD32, CLEA Japan) from 4 weeks of age. At 5 weeks of age, animals were treated with PF-06427878 at 2 or 20 mg/kg BID (4 or 40 mg/kg per day) or vehicle alone (1% methylcellulose/80 mM tris with 0.5% hypromellose acetate succinate) for 4 weeks. Details of disease progression in this model can be found elsewhere (*19*). Mice were euthanized at 9 weeks of age by exsanguination through direct cardiac puncture under ether anesthesia, and the livers were collected for histopathological analysis, specifically H&E and Sirius red staining, and gene expression. For H&E staining, sections were cut from paraffin blocks of liver tissue prefixed in Bouin's solution and stained with Lillie-Mayer's hematoxylin (Muto Pure Chemicals Co.) and Eosin solution (Wako Pure Chemical Industries). NAFLD activity score was calculated according to the criteria of Kleiner *et al.* (*20*). To visualize collagen deposition, we stained Bouin's fixed liver sections using picro-Sirius red solution (Waldeck GmbH & Co.). For quantitative analysis, bright-field images of Sirius red–stained sections were captured around the central vein using a digital camera (DFC280, Leica) at 200-fold magnification, and the positive areas in five fields/sections were measured using ImageJ software (National Institutes of Health). A gene expression analysis was performed ostensibly as described for the WTD rat model (see the Supplementary Materials).

Animal models and ethics statement. All activities involving animals in the United States were carried out in Association for Assessment and Accreditation of Laboratory Animal Care International–accredited facilities and in accordance with federal, state, local, and institutional guidelines governing the use of laboratory animals in research and were reviewed and approved by Pfizer Institutional Animal Care and Use Committees (or other) in compliance with the *Guide for the Care and Use of Laboratory Animals*, eight edition (*49*). STAM NASH model mice were housed and cared for in accordance with the Japanese Pharmacological Society Guidelines for Animal Use.

Phase 1 clinical studies

We evaluated the safety, tolerability, and pharmacodynamic effects of PF-06427878 in phase 1 clinical studies B7871002 and B7871005. Study B7871002 was conducted at a single center in Belgium (Pfizer's Clinical Research Unit, Brussels), and study B7871005 was conducted at two centers in the United States (PAREXEL International, Glendale, CA and QPS Miami Research Associates, Miami, FL). Both studies (fig. S3) randomized healthy adult participants between the ages of 18 and 55 years; however, in study B7871002, the eligible population was limited to a BMI of 17.5 to 35.4 kg/m^2, whereas in study B7871005, the eligible population was broadened to include a BMI of ≥25 kg/m^2. PF-06427878 or matching placebo was administered more than 14 days of inpatient stays, with witnessed dosing under double-blind conditions in sequential cohorts. In study B7871002, up to two participants were randomized to placebo, and up to eight participants were randomized to PF-06427878 (15, 45, 150, or 450 mg/day, daily administration divided Q8H with a meal) in each cohort. In study B7871005, participants were randomized in a 1:1 ratio to receive placebo or PF-06427878 1500 mg/day, daily administration divided Q8H with a meal. In both studies, sample sizes were chosen empirically to minimize exposure to a new chemical entity yet provide adequate safety, tolerability, and pharmacodynamics data at each dose.

Both studies were conducted in compliance with the ethical principles of the Declaration of Helsinki and International Conference on Harmonization Good Clinical Practice guidelines. The protocols for studies B7871002 and B7871005 were approved by the Independent Ethics Committee and Institutional Review Board, respectively, at the investigational centers. All adult participants provided informed consent.

Given the short plasma pharmacokinetic half-life of PF-06427878 after single oral doses of ≥100 mg (3.0 to 5.3 hours; study B7871001), Q8H dosing with food was chosen for studies B7871002 and B7871005. The safety, pharmacokinetic, and pharmacodynamic results from study B7871001 were used to establish the starting dose of 15 mg/day in study B7871002, with no more than a half-log (~3.5-fold) increase

for each dose escalation to the top dose of 450 mg/day. Study B7871005 was an extension of study B7871002 with a dosing regimen of 1500 mg/day evaluated. Safety was assessed by reported adverse events, physical examination, supine vital signs, supine electrocardiograms, and clinical laboratory tests including hematology, clinical chemistry, and urinalysis.

Blood samples for serum analysis of hepatic biomarkers were taken at various time points in both studies. ALT, AST, ALP, and TBILI concentrations were assessed on days −1 (study B7871002 only), 0, 1, 4, 7, 10, and 14. Fasted lipid profiles (TG, LDL-c, HDL-c, and TC) were assessed on days −1 (study B7871002 only), 0, 1, 2, 4, 7, 10, 14, and 15, with blood samples collected after an overnight fast of at least 7.5 hours. In addition, in study B7871005, postprandial assessments were also performed for TG concentrations on days 0 and 14, with liver fat measured by MRI-PDFF on days −1 and 15. The imaging assessment used a validated, two-dimensional, six echo spoiled-gradient-recalled-echo breath-hold pulse sequences (*52*) standardized across sites. Analysis was performed by a central reader, blinded to treatment assignment, applying 2.5-cm-diameter regions of interest on each of nine anatomical liver segments, excepting one segment (the caudate) in which a region with a diameter of 1.5 cm was identified.

Statistical analyses

Data on TG concentrations and expression of lipogenic genes in WTD-fed rats and on the development of liver disease in the STAM NASH-HCC mouse model were analyzed by one-way analysis of variance (ANOVA), followed by Dunnett's multiple comparison test. In studies B7871002 and B7871005, individual changes from baseline at end of study (that is, value at day 14 compared with value at baseline) in markers of liver function (ALT, AST, ALP, and TBILI) were calculated. Assuming a monotonic response, the effect of the dose on the mean level of these liver function tests was analyzed using Williams' test, with statistical significance defined as $P < 0.05$.

We analyzed TG concentrations, serum lipid concentrations, and natural log-transformed individual relative changes from baseline at end of study (average of values on days 14 and 15/ average of values on days 0 and 1) were analyzed using a mixed-effect model with dosing regimen as a fixed effect and participant as a random effect. Least squares (LS) estimates and their 80% confidence intervals were reported and exponentiated (back transformed). The back-transformed relative change and ratio of adjusted geometric means were transformed to percent change as follows: Percent change = 100 × (Relative change − 1). *P* values were calculated from the differences between placebo and active treatment group LS means in the logarithmic scale.

SUPPLEMENTARY MATERIALS

stm.sciencemag.org/cgi/content/full/11/520/eaav9701/DC1
Materials and Methods
Fig. S1. Chemical structure of PF-06427878.
Fig. S2. Effect of PF-06427878 on circulating hepatic biomarkers in Wistar Han IGS rats and cynomolgus monkeys in 2-week toxicology studies.
Fig. S3. Subject disposition in clinical studies of PF-06427878 in healthy humans.
Fig. S4. Descriptive summary (*n*, means, and SEM) and individual participant–level MRI-PDFF data for liver fat in humans (study B7871005).
Table S1. Effect of PF-06427878 on selected clinical chemistry parameters in the STAM mouse model of NASH.
Table S2. Effect of PF-06427878 on fasting serum lipids on day 14 in studies B7871002 and B7871005.
Data file S1. Raw data from nonclinical in vivo studies.

View/request a protocol for this paper from *Bio-protocol*.

REFERENCES AND NOTES

1. Review Team, D. R. LaBrecque, Z. Abbas, F. Anania, P. Ferenci, A. G. Khan, K. L. Goh, S. S. Hamid, V. Isakov, M. Lizarzabal, M. M. Peñaranda, J. F. Ramos, S. Sarin, D. Stimac, A. B. Thomson, M. Umar, J. Krabshuis, A. LeMair; World Gastroenterology Organisation, World Gastroenterology Organisation global guidelines: Nonalcoholic fatty liver disease and nonalcoholic steatohepatitis. *J. Clin. Gastroenterol.* **48**, 467–473 (2014).
2. Z. M. Younossi, A. B. Koenig, D. Abdelatif, Y. Fazel, L. Henry, M. Wymer, Global epidemiology of nonalcoholic fatty liver disease—Meta-analytic assessment of prevalence, incidence, and outcomes. *Hepatology* **64**, 73–84 (2016).
3. E. M. Brunt, D. G. Tiniakos, Histopathology of nonalcoholic fatty liver disease. *World J. Gastroenterol.* **16**, 5286–5296 (2010).
4. A. M. Diehl, C. Day, Cause, pathogenesis, and treatment of nonalcoholic steatohepatitis. *N. Engl. J. Med.* **377**, 2063–2072 (2017).
5. A. J. Sanyal, S. L. Friedman, A. J. McCullough, L. Dimick-Santos, Challenges and opportunities in drug and biomarker development for nonalcoholic steatohepatitis: Findings and recommendations from an American Association for the Study of Liver Diseases (AASLD)–U.S. Food and Drug Administration joint workshop. *Hepatology* **61**, 1392–1405 (2015).
6. F. Z. Khan, R. B. Perumpail, R. J. Wong, A. Ahmed, Advances in hepatocellular carcinoma: Nonalcoholic steatohepatitis-related hepatocellular carcinoma. *World J. Hepatol.* **7**, 2155–2161 (2015).
7. B. A. Neuschwander-Tetri, Hepatic lipotoxicity and the pathogenesis of nonalcoholic steatohepatitis: The central role of nontriglyceride fatty acid metabolites. *Hepatology* **52**, 774–788 (2010).
8. C.-L. E. Yen, S. J. Stone, S. Koliwad, C. Harris, R. V. Farese Jr., *Thematic review series*: Glycerolipids. DGAT enzymes and triacylglycerol biosynthesis. *J. Lipid. Res.* **49**, 2283–2301 (2008).
9. V. A. Zammit, Hepatic triacylglycerol synthesis and secretion: DGAT2 as the link between glycaemia and triglyceridaemia. *Biochem. J.* **451**, 1–12 (2013).
10. S. Cases, S. J. Stone, P. Zhou, E. Yen, B. Tow, K. D. Lardizabal, T. Voelker, R. V. Farese Jr., Cloning of DGAT2, a second mammalian diacylglycerol acyltransferase, and related family members. *J. Biol. Chem.* **276**, 38870–38876 (2001).
11. K. Futatsugi, D. W. Kung, S. T. Orr, S. Cabral, D. Hepworth, G. Aspnes, S. Bader, J. Bian, M. Boehm, P. A. Carpino, S. B. Coffey, M. S. Dowling, M. Herr, W. Jiao, S. Y. Lavergne, Q. Li, R. W. Clark, D. M. Erion, K. Kou, K. Lee, B. A. Pabst, S. M. Perez, J. Purkal, C. C. Jorgensen, T. C. Goosen, J. R. Gosset, M. Niosi, J. C. Pettersen, J. A. Pfefferkorn, K. Ahn, B. Goodwin, Discovery and optimization of imidazopyridine-based inhibitors of diacylglycerol acyltransferase 2 (DGAT2). *J. Med. Chem.* **58**, 7173–7185 (2015).
12. K. Yamaguchi, L. Yang, S. McCall, J. Huang, X. X. Yu, S. K. Pandey, S. Bhanot, B. P. Monia, Y.-X. Li, A. M. Diehl, Inhibiting triglyceride synthesis improves hepatic steatosis but exacerbates liver damage and fibrosis in obese mice with nonalcoholic steatohepatitis. *Hepatology* **45**, 1366–1374 (2007).
13. U. Risérus, D. Sprecher, T. Johnson, E. Olson, S. Hirschberg, A. Liu, Z. Fang, P. Hegde, D. Richards, L. Sarov-Blat, J. C. Strum, S. Basu, J. Cheeseman, B. A. Fielding, S. M. Humphreys, T. Danoff, N. R. Moore, P. Murgatroyd, S. O'Rahilly, P. Sutton, T. Willson, D. Hassall, K. N. Frayn, F. Karpe, Activation of peroxisome proliferator-activated receptor (PPAR)δ promotes reversal of multiple metabolic abnormalities, reduces oxidative stress, and increases fatty acid oxidation in moderately obese men. *Diabetes* **57**, 332–339 (2008).
14. C. S. Choi, D. B. Savage, A. Kulkarni, X. X. Yu, Z.-X. Liu, K. Morino, S. Kim, A. Distefano, V. T. Samuel, S. Neschen, D. Zhang, A. Wang, X.-M. Zhang, M. Kahn, G. W. Cline, S. K. Pandey, J. G. Geisler, S. Bhanot, B. P. Monia, G. I. Shulman, Suppression of diacylglycerol acyltransferase-2 (*DGAT2*), but not *DGAT1*, with antisense oligonucleotides reverses diet-induced hepatic steatosis and insulin resistance. *J. Biol. Chem.* **282**, 22678–22688 (2007).
15. X. X. Yu, S. F. Murray, S. K. Pandey, S. L. Booten, D. Bao, X.-Z. Song, S. Kelly, S. Chen, R. McKay, B. P. Monia, S. Bhanot, Antisense oligonucleotide reduction of DGAT2 expression improves hepatic steatosis and hyperlipidemia in obese mice. *Hepatology* **42**, 362–371 (2005).
16. S. Cabral, K. Futatsugi, D. Hepworth, K. Huard, D. W. Kung, S. T. M. Orr, K. Song, Diacylglycerol acyltransferase 2 inhibitors, U.S. Patent 9,440,949 (2015).
17. C. Li, L. Li, J. Lian, R. Watts, R. Nelson, B. Goodwin, R. Lehner, Roles of acyl-CoA:diacylglycerol acyltransferases 1 and 2 in triacylglycerol synthesis and secretion in primary hepatocytes. *Arterioscler. Thromb. Vasc. Biol.* **35**, 1080–1091 (2015).
18. S. Romeo, J. Kozlitina, C. Xing, A. Pertsemlidis, D. Cox, L. A. Pennacchio, E. Boerwinkle, J. C. Cohen, H. H. Hobbs, Genetic variation in *PNPLA3* confers susceptibility to nonalcoholic fatty liver disease. *Nat. Genet.* **40**, 1461–1465 (2008).
19. J. S. Millar, D. A. Cromley, M. G. McCoy, D. J. Rader, J. T. Billheimer, Determining hepatic triglyceride production in mice: Comparison of poloxamer 407 with Triton WR-1339. *J. Lipid Res.* **46**, 2023–2028 (2005).
20. C. E. Chandler, D. E. Wilder, J. L. Pettini, Y. E. Savoy, S. F. Petras, G. Chang, J. Vincent, H. J. Harwood Jr., CP-346086: An MTP inhibitor that lowers plasma cholesterol and triglycerides in experimental animals and in humans. *J. Lipid Res.* **44**, 1887–1901 (2003).

21. M. Fujii, Y. Shibazaki, K. Wakamatsu, Y. Honda, Y. Kawauchi, K. Suzuki, S. Arumugam, K. Watanabe, T. Ichida, H. Asakura, H. Yoneyama, A murine model for non-alcoholic steatohepatitis showing evidence of association between diabetes and hepatocellular carcinoma. *Med. Mol. Morphol.* **46**, 141–152 (2013).
22. D. E. Kleiner, E. M. Brunt, M. Van Natta, C. Behling, M. J. Contos, O. W. Cummings, L. D. Ferrell, Y.-C. Liu, M. S. Torbenson, A. Unalp-Arida, M. Yeh, A. J. McCullough, A. J. Sanyal; Nonalcoholic Steatohepatitis Clinical Research Network, Design and validation of a histological scoring system for nonalcoholic fatty liver disease. *Hepatology* **41**, 1313–1321 (2005).
23. T. Higashi, S. L. Friedman, Y. Hoshida, Hepatic stellate cells as key target in liver fibrosis. *Adv. Drug Deliv. Rev.* **121**, 27–42 (2017).
24. R. C. Benyon, J. P. Iredale, S. Goddard, P. J. Winwood, M. J. Arthur, Expression of tissue inhibitor of metalloproteinases 1 and 2 is increased in fibrotic human liver. *Gastroenterology* **110**, 821–831 (1996).
25. D. C. Rockey, N. Weymouth, Z. Shi, Smooth muscle α actin (*Acta2*) and myofibroblast function during hepatic wound healing. *PLOS ONE* **8**, e77166 (2013).
26. G. S. Baroni, L. D'Ambrosio, P. Curto, A. Casini, R. Mancini, A. M. Jezequel, A. Benedetti, Interferon gamma decreases hepatic stellate cell activation and extracellular matrix deposition in rat liver fibrosis. *Hepatology* **23**, 1189–1199 (1996).
27. NCD Risk Factor Collaboration (NCD-RisC), Worldwide trends in body-mass index, underweight, overweight, and obesity from 1975 to 2016: A pooled analysis of 2416 population-based measurement studies in 128.9 million children, adolescents, and adults. *Lancet* **390**, 2627–2642 (2017).
28. G. Marchesini, M. Brizi, G. Bianchi, S. Tomassetti, E. Bugianesi, M. Lenzi, A. J. McCullough, S. Natale, G. Forlani, N. Melchionda, Nonalcoholic fatty liver disease: A feature of the metabolic syndrome. *Diabetes* **50**, 1844–1850 (2001).
29. P. Socha, A. Wierzbicka, J. Neuhoff-Murawska, D. Włodarek, J. Podleśny, J. Socha, Nonalcoholic fatty liver disease as a feature of the metabolic syndrome. *Rocz. Panstw. Zakl. Hig.* **58**, 129–137 (2007).
30. N. Tsuda, S. Kumadaki, C. Higashi, M. Ozawa, M. Shinozaki, Y. Kato, K. Hoshida, S. Kikuchi, Y. Nakano, Y. Ogawa, S. Furusako, Intestine-targeted DGAT1 inhibition improves obesity and insulin resistance without skin aberrations in mice. *PLOS ONE* **9**, e112027 (2014).
31. J. Cao, Y. Zhou, H. Peng, X. Huang, S. Stahler, V. Suri, A. Qadri, T. Gareski, J. Jones, S. Hahm, M. Perreault, J. McKew, M. Shi, X. Xu, J. F. Tobin, R. E. Gimeno, Targeting Acyl-CoA:Diacylglycerol acyltransferase 1 (DGAT1) with small molecule inhibitors for the treatment of metabolic diseases. *J. Biol. Chem.* **286**, 41838–41851 (2011).
32. J. Chen, D. Meyers, D. Keefe, J. Yu, G. Sunkara, Clinical pharmacokinetics of pradigastat, a novel diacylglycerol acyltransferase 1 inhibitor. *J. Drug Des. Res.* **4**, 1044 (2017).
33. X. S. Song, J. Zhang, X. Chen, O. Palyha, C. Chung, L. M. Sonatore, L. Wilsie, S. Stout, D. G. McLaren, A. Taggart, J. E. Imbriglio, S. Pinto, M. Garcia-Calvo, G. H. Addona, Identification of DGAT2 inhibitors using mass spectrometry. *J. Biomol. Screen.* **21**, 117–126 (2016).
34. D. G. McLaren, S. Han, B. A. Murphy, L. Wilsie, S. J. Stout, H. Zhou, T. P. Roddy, J. N. Gorski, D. E. Metzger, M. K. Shin, D. F. Reilly, H. H. Zhou, M. Tadin-Strapps, S. R. Bartz, A. M. Cumiskey, T. H. Graham, D. M. Shen, K. O. Akinsanya, S. F. Previs, J. E. Imbriglio, S. Pinto, DGAT2 inhibition alters aspects of triglyceride metabolism in rodents but not in non-human primates. *Cell Metab.* **27**, 1236–1248.e6 (2018).
35. B. Pabst, K. Futatsugi, Q. Li, K. Ahn, Mechanistic characterization of long residence time inhibitors of diacylglycerol acyltransferase 2 (DGAT2). *Biochemistry* **57**, 6997–7010 (2018).
36. N. Sattar, E. Forrest, D. Preiss, Non-alcoholic fatty liver disease. *BMJ* **349**, g4596 (2014).
37. G. Marchesini, S. Moscatiello, S. Di Domizio, G. Forlani, Obesity-associated liver disease. *J. Clin. Endocrinol. Metab.* **93**, S74–S80 (2008).
38. D. Sorbi, J. Boynton, K. D. Lindor, The ratio of aspartate aminotransferase to alanine aminotransferase: Potential value in differentiating nonalcoholic steatohepatitis from alcoholic liver disease. *Am. J. Gastroenterol.* **94**, 1018–1022 (1999).
39. C. D. Meyers, M. Serrano-Wu, A. Ahmed, J. Chen, E. Rocheford, R. Commerford, B. Hubbard, M. Brousseau, L. Li, P. Meihui, R. Chatelain, B. Dardik, The DGAT1 inhibitor pradigastat decreases chylomicron secretion and prevents postprandial triglyceride elevation in humans. *J. Clin. Lipidol.* **7**, 285 (2013).
40. A. J. Sanyal, K. Cusi, S. Patel, M. Wright, C. Liu, D. L. Keefe, Effect of pradigastat, a diacylglycerol acyltransferase 1 inhibitor, on liver fat content in nonalcoholic fatty liver disease: 2147. *Hepatology* **62**, 1253A (2015).
41. E. S. G. Stroes, S. Patel, S. Bernelot-Moens, Y. Zhou, D. Keefe, M. Wright, D. Gaudet, The diacylglycerol acyltransferase 1 inhibitor, pradigastat, was well tolerated in a 52-week clinical trial in FCS patients. *J. Clin. Lipidol.* **9**, 450 (2015).
42. H. Denison, C. Nilsson, L. Löfgren, A. Himmelmann, G. Mårtensson, M. Knutsson, A. Al-Shurbaji, H. Tornqvist, J. W. Eriksson, Diacylglycerol acyltransferase 1 inhibition with AZD7687 alters lipid handling and hormone secretion in the gut with intolerable side effects: A randomized clinical trial. *Diabetes Obes. Metab.* **16**, 334–343 (2014).
43. S. Cases, S. J. Smith, Y.-W. Zheng, H. M. Myers, S. R. Lear, E. Sande, S. Novak, C. Collins, C. B. Welch, A. J. Lusis, S. K. Erickson, R. V. Farese Jr., Identification of a gene encoding an acyl CoA:diacylglycerol acyltransferase, a key enzyme in triacylglycerol synthesis. *Proc. Natl. Acad. Sci. U.S.A.* **95**, 13018–13023 (1998).
44. X. Lu, G. M. Peloso, D. J. Liu, Y. Wu, H. Zhang, W. Zhou, J. Li, C. S. Tang, R. Dorajoo, H. Li, J. Long, X. Guo, M. Xu, C. N. Spracklen, Y. Chen, X. Liu, Y. Zhang, C. C. Khor, J. Liu, L. Sun, L. Wang, Y. T. Gao, Y. Hu, K. Yu, Y. Wang, C. Y. Y. Cheung, F. Wang, J. Huang, Q. Fan, Q. Cai, S. Chen, J. Shi, X. Yang, W. Zhao, W. H. Sheu, S. S. Cherny, M. He, A. B. Feranil, L. S. Adair, P. Gordon-Larsen, S. Du, R. Varma, Y. I. Chen, X. O. Shu, K. S. L. Lam, T. Y. Wong, S. K. Ganesh, Z. Mo, K. Hveem, L. G. Fritsche, J. B. Nielsen, H. F. Tse, Y. Huo, C. Y. Cheng, Y. E. Chen, W. Zheng, E. S. Tai, W. Gao, X. Lin, W. Huang, G. Abecasis, G. Consortium, S. Kathiresan, K. L. Mohlke, T. Wu, P. C. Sham, D. Gu, C. J. Willer, Exome chip meta-analysis identifies novel loci and East Asian-specific coding variants that contribute to lipid levels and coronary artery disease. *Nat. Genet.* **49**, 1722–1730 (2017).
45. K. E. Corey, R. Vuppalanchi, L. A. Wilson, O. W. Cummings, N. Chalasani; Nash CRN, NASH resolution is associated with improvements in HDL and triglyceride levels but not improvement in LDL or non-HDL-C levels. *Aliment. Pharmacol. Ther.* **41**, 301–309 (2015).
46. A. M. Lincoff, S. J. Nicholls, J. S. Riesmeyer, P. J. Barter, H. B. Brewer, K. A. A. Fox, C. M. Gibson, C. Granger, V. Menon, G. Montalescot, D. Rader, A. R. Tall, E. McErlean, K. Wolski, G. Ruotolo, B. Vangerow, G. Weerakkody, S. G. Goodman, D. Conde, D. K. McGuire, J. C. Nicolau, J. L. Leiva-Pons, Y. Pesant, W. Li, D. Kandath, S. Kouz, N. Tahirkheli, D. Mason, S. E. Nissen; Accelerate Investigators, Evacetrapib and cardiovascular outcomes in high-risk vascular disease. *N. Engl. J. Med.* **376**, 1933–1942 (2017).
47. R. Loomba, E. Morgan, M. Fung, L. Watts, R. Geary, S. Bhanot, PS-106-an international, randomized, placebo-controlled phase 2 trial demonstrates novel effects of DGAT2 antisense inhibition in reducing steatosis without causing hypertriglyceridemia in T2DM patients. *J. Hepatol.* **70**, e67–e68 (2019).
48. A. Mardinoglu, H. Wu, E. Bjornson, C. Zhang, A. Hakkarainen, S. M. Räsänen, S. Lee, R. M. Mancina, M. Bergentall, K. H. Pietiläinen, S. Söderlund, N. Matikainen, M. Ståhlman, P. O. Bergh, M. Adiels, B. D. Piening, M. Granér, N. Lundbom, K. J. Williams, S. Romeo, J. Nielsen, M. Snyder, M. Uhlén, G. Bergström, R. Perkins, H.-U. Marschall, F. Bäckhed, M.-R. Taskinen, J. Borén, An integrated understanding of the rapid metabolic benefits of a carbohydrate-restricted diet on hepatic steatosis in humans. *Cell Metab.* **27**, 559–571.e5 (2018).
49. Z. Permutt, T.-A. Le, M. R. Peterson, E. Seki, D. A. Brenner, C. Sirlin, R. Loomba, Correlation between liver histology and novel magnetic resonance imaging in adult patients with non-alcoholic fatty liver disease – MRI accurately quantifies hepatic steatosis in NAFLD. *Aliment. Pharmacol. Ther.* **36**, 22–29 (2012).
50. S. Jayakumar, M. S. Middleton, E. J. Lawitz, P. S. Mantry, S. H. Caldwell, H. Arnold, A. Mae Diehl, R. Ghalib, M. Elkhashab, M. F. Abdelmalek, K. V. Kowdley, C. Stephen Djedjos, R. Xu, L. Han, G. Mani Subramanian, R. P. Myers, Z. D. Goodman, N. H. Afdhal, M. R. Charlton, C. B. Sirlin, R. Loomba, Longitudinal correlations between MRE, MRI-PDFF, and liver histology in patients with non-alcoholic steatohepatitis: Analysis of data from a phase II trial of selonsertib. *J. Hepatol.* **70**, 133–141 (2019).
51. M. Monetti, M. C. Levin, M. J. Watt, M. P. Sajan, S. Marmor, B. K. Hubbard, R. D. Stevens, J. R. Bain, C. B. Newgard, R. V. Farese Sr., A. L. Hevener, R. V. Farese Jr., Dissociation of hepatic steatosis and insulin resistance in mice overexpressing DGAT in the liver. *Cell Metab.* **6**, 69–78 (2007).
52. A. Mashhood, R. Railkar, T. Yokoo, Y. Levin, L. Clark, S. Fox-Bosetti, M. S. Middleton, J. Riek, E. Kauh, B. J. Dardzinski, D. Williams, C. Sirlin, N. J. Shire, Reproducibility of hepatic fat fraction measurement by magnetic resonance imaging. *J. Magn. Reson. Imaging* **37**, 1359–1370 (2013).

Acknowledgments: We thank the healthy adults who participated in the studies presented, the investigators and site coordinators, the expertise offered by C. Houle in identifying representative images of the pathology depicted in Fig. 3, as well as the constructive input offered by R. Dullea and M. Birnbaum. Editorial support was provided by K. Woollcott, on behalf of CMC CONNECT, a division of Complete Medical Communications Ltd., Glasgow, UK, and the editorial services were funded by Pfizer Inc., New York, NY, USA in accordance with Good Publication Practice (GPP3) guidelines. **Funding:** The work presented here was funded by Pfizer Inc. **Author contributions:** N.B.A. led the design and conduct of all clinical studies, as well as the development of this manuscript from outline to the expanded version presented herein. S.C.-G. verified all data and carried out/supervised the statistical analyses presented in this publication. J.P. was primarily responsible for all nonclinical work. T.Z. participated in the acquisition of all clinical data. C.C. helped design, execute, and run downstream analysis (quantitative polymerase chain reaction and plasma analysis) of the rat Western diet experiment. S.P. participated in the acquisition and analysis of all nonclinical data. K.C. participated in the design of all reported clinical experiments. B.G. designed all nonclinical studies, provided input on the design of the clinical studies, and prepared Figs. 1 and 2. All authors contributed to data interpretation, critically reviewed each manuscript draft, provided approval of the final version to be published, and accepted accountability for all aspects of the work. **Competing interests:** All authors were employees of Pfizer Inc. at the time the work

summarized in this paper was conducted; they may own stock or stock options in Pfizer Inc. B.G. is currently an employee of Enanta Pharmaceuticals, Inc. J.P. is currently an employee of AbbVie Pharmaceuticals, Inc. **Data and materials availability:** All data associated with this study are present in the paper or the Supplementary Materials. Upon request and subject to certain criteria, conditions, and exceptions (see https://pfizer.com/science/clinical-trials/trial-data-and-results for more information), Pfizer will provide access to individual deidentified participant data from Pfizer-sponsored global interventional clinical studies conducted for medicines, vaccines, and medical devices (i) for indications that have been approved in the United States or European Union or (ii) in programs that have been terminated (that is, development for all indications has been discontinued). Pfizer will also consider requests for the protocols, datasets, and statistical analysis plans of studies NCT02855177 and NCT2391623. Data from these trials may be requested 24 months after study completion. The deidentified participant data will be made available to researchers whose proposals meet the research criteria and other conditions, and for which an exception does not apply, via a secure portal. To gain access, data requestors must enter into a data access agreement with Pfizer (see https://vivli.org/resources/vivli-data-use-agreement-2/ for a copy of this agreement). Upon request and subject to certain criteria, conditions, and exceptions (see https://pfizer.com/science/collaboration/compound-transfer-program for more information), PF-06427878 is available from Pfizer under a Compound Transfer Agreement. Requests for Pfizer compounds can be submitted at https://iirsubmission.pfizer.com/. The clinical trials (NCT02855177 and NCT02391623) are registered at www.clinicaltrials.gov.

Submitted 6 November 2018
Resubmitted 25 February 2019
Accepted 8 November 2019
Published 27 November 2019
10.1126/scitranslmed.aav9701

Citation: N. B. Amin, S. Carvajal-Gonzalez, J. Purkal, T. Zhu, C. Crowley, S. Perez, K. Chidsey, A. M. Kim, B. Goodwin, Targeting diacylglycerol acyltransferase 2 for the treatment of nonalcoholic steatohepatitis. *Sci. Transl. Med.* **11**, eaav9701 (2019).

Science Translational Medicine

Targeting diacylglycerol acyltransferase 2 for the treatment of nonalcoholic steatohepatitis

Neeta B. Amin, Santos Carvajal-Gonzalez, Julie Purkal, Tong Zhu, Collin Crowley, Sylvie Perez, Kristin Chidsey, Albert M. Kim and Bryan Goodwin

Sci Transl Med **11**, eaav9701.
DOI: 10.1126/scitranslmed.aav9701

A pill a day keeps liver fat away

Nonalcoholic fatty liver diseases can progress to liver failure but currently lack approved treatments. Amin *et al.* tested the therapeutic efficacy of a small-molecule inhibitor of diacylglycerol acyltransferase 2 (DGAT2; responsible for hepatic triglyceride production) in rodent models of nonalcoholic steatohepatitis and found that PF-06427878 improved liver steatosis and function. Two phase 1 clinical trials in healthy humans showed improved markers of liver function at the highest dose administered. One of the clinical trials measured liver fat and demonstrated its reduction in healthy participants on the highest dose. PF-06427878 may be a candidate to treat conditions related to fatty liver in humans.